

Age, geochemistry and Sr-Nd-Pb isotopic compositions of alkali volcanic rocks from Mt. Melbourne and the western Ross Sea, Antarctica

Mi Jung Lee*
Jong Ik Lee
Tae Hoon Kim
Joohan Lee
Keisuke Nagao

} Division of Polar Earth System Sciences, Korea Polar Research Institute (KOPRI), Incheon 406-840, Republic of Korea

ABSTRACT: New K/Ar ages and geochemical and isotope data (Sr, Nd, Pb) of submarine samples from the Terror Rift Region and subaerial lavas from Mt. Melbourne Volcanic Field (MMVF) in the western Ross Sea, Antarctica, are presented. The MMVF samples are classified into Groups A and B based on their temporal and spatial distribution. All samples are alkaline, ranging from basanite to trachybasalt, and exhibit the Ocean Island Basalt (OIB)-like patterns of trace element distribution, with a prominent depletion in K and Pb. New K/Ar ages and geochemical data of the studied samples show no correlations between age and their compositions and suggest that they represent products of three different magmatic episodes. The Terror Rift submarine lavas (0.46–0.57 Ma) display a distinct trend, with more primitive geochemical characteristics (higher MgO (7.2–9.8 wt%) and CaO (9.9–11.9 wt%) and stronger HIMU signature (higher $^{206}\text{Pb}/^{204}\text{Pb}$ and $^{143}\text{Nd}/^{144}\text{Nd}$ ratios, and less radiogenic $^{87}\text{Sr}/^{86}\text{Sr}$) than those of MMVF basalts. Results from a rare earth element (REE) model suggest that the Terror Rift submarine lavas are derived from small degrees (1–2%) of partial melting of an amphibole-bearing garnet peridotite mantle source. Despite the distinctly different ages and locations of the MMVF Group A (0.16–0.33 Ma) and B (1.25–1.34 Ma) basalts, they show similar geochemical and isotopic features, indicating the sharing of common mantle sources and magma processes during magma generation. Incompatible trace element ratios (e.g., Ba/Nb = 6.4–13.2, La/Yb_N = 14.4–23.2, Dy/Yb = 2.2–3.0) and isotopic compositions of the MMVF Group A and B volcanics suggest derivation from higher degrees (2–5%) of partial melting of an amphibole bearing garnet peridotite source and strong influence of an EMI-type mantle source. The stronger HIMU signature of the Terror Rift submarine lavas appears to be related to smaller degrees of partial melting, suggesting predominant contribution of the HIMU component to the less partially melted rocks from the Cenozoic NVL magmatism. In contrast, the higher degree of MMVF A and B magmas can be explained by greater interaction with heterogeneous lithospheric mantle, resulting in a diluted HIMU signature compared with that of the Terror Rift submarine lavas. We assume that HIMU- and EMI-type mantle components incorporated in the Cenozoic NVL magmas originated from sub-continental lithospheric mantle metasomatized by plume or subduction-related fluids prior to the breakup of Gondwanaland.

Key words: Terror Rift submarine lavas, Mt. Melbourne Volcanic Field, Sr-Nd-Pb isotope, K/Ar ages, Antarctica

1. INTRODUCTION

Continental rift systems are frequently associated with abundant magmatism. The thinning of the continental lithosphere and transitional decompression or heating by rising asthenospheric mantle during the rifting process are believed to be important causes of magma generation (McKenzie and Bickle, 1988). Magmas erupted in these settings are characterized by Ocean Island Basalt (OIB)-like patterns of trace element distribution and radiogenic isotopic compositions. Despite the geochemical similarities of OIB and continental rift basalts, the source and origin of continental rift basalts variously interpreted as of lithospheric origin (Wilson and Patterson, 2001; Weinstein et al., 2006; Ma et al., 2011), asthenospheric origin (Aldanmaz et al., 2000, 2006), or the interaction of both (Johnson et al., 2005; Yan and Zhao, 2008). Specially, metasomatized subcontinental lithospheric mantle (SCLM) is assumed to be one of the crucial source components to their genesis (DePaolo and Daley, 2000; Sprung et al., 2007; Nardini et al., 2009). The explanation of the nature of the mantle sources within the framework of geochemical-tectonic evolution of these sources is still a matter of significant debate.

The West Antarctic Rift System (WARS) is one of the most active continental rift zones on Earth and is characterized by a topographical trough 750–1000 km wide and 3000 km long, running from the Antarctic Peninsula to the Ross Sea Embayment, Northern Victoria Land (NVL, Fig. 1, Behrendt, 1999). During the Cenozoic, continental rift basalts related to WARS erupted intermittently in NVL (from ~48 Ma, Rocchi et al., 2002) and Marie Byrd Land (from ~30 Ma, Hart et al., 1997), comprising a volume of more than 10^6 km^3 (Behrendt, 1999). A number of geological and geochemical studies have been carried out on these basalts to decipher their origin (Behrendt et al., 1991; Hole and LeMasurier, 1994; Rocholl et al., 1995; LeMasurier and Landis, 1996; Hart et al., 1997; Storey et al., 1999; Panter et al., 2000, 2006; Rocchi et al., 2002, 2003, 2005; Finn et al., 2005; Nardini et al.,

*Corresponding author: mjlee@kopri.re.kr

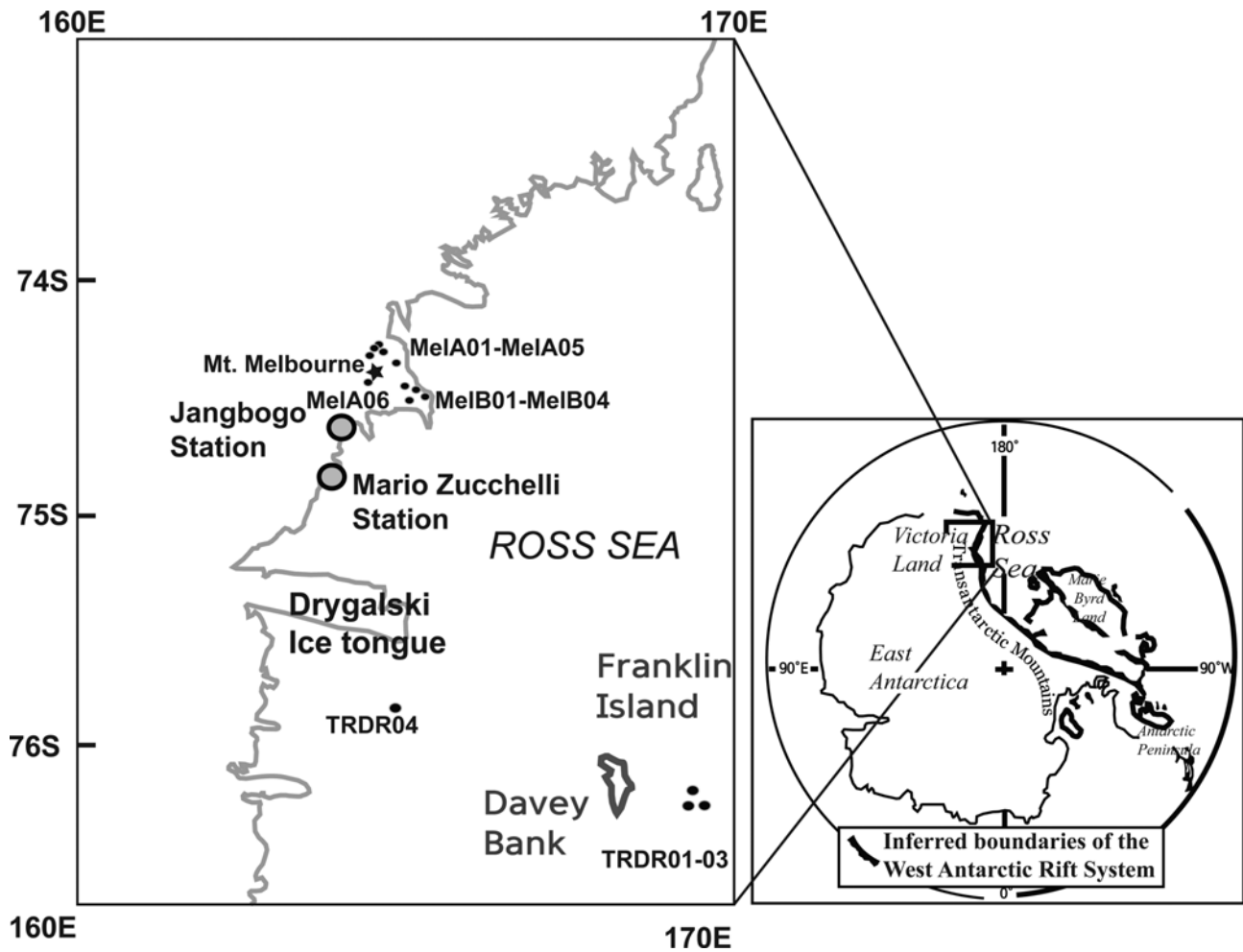


Fig. 1. Regional sketch map of Antarctica showing the boundaries of the West Antarctic Rift System and Northern Victoria Land. The enlarged area shows sampling sites.

2009). The proposed models include a plume source, which was favored in the early literature (Behrendt et al., 1991; Hole and LeMasurier, 1994; LeMasurier and Landis, 1996; Storey et al., 1999), whereas more recently, decompression melting of metasomatized lithospheric mantle in a transtensive tectonic regime during Cretaceous amagmatic extensional rifting has been favored (Rocchi et al., 2005; Finn et al., 2005; Panter et al., 2006; Nardini et al., 2009).

Previous studies are biased toward data gathered from Cenozoic basalts in Marie Byrd Land (Hart et al., 1995, 1997; Panter et al., 2000; Ryan and Kyle, 2004) and several distinct regions of Northern and Southern Victoria Land (Cooper et al., 2007; Nardini et al., 2009; Sims et al., 2008; 2013; Martin et al., 2013). There are few studies of Pb isotopic compositions in Mt. Melbourne Volcanic Field (MMVF) basalts. Rocholl et al. (1995) and Rocchi et al. (2000) generated Sr and Nd isotope data for volcanic and plutonic samples from NVL. Nardini et al. (2009) reported Pb isotopes for several primitive basaltic samples from NVL. In this paper, we report new Pb isotope data corrected for mass fractionation by double-

spike techniques, together with Sr-Nd and K/Ar geochronological data for previously unsampled submarine lavas from the Terror Rift Region of the Ross Sea as well as additional samples from the MMVF. The purposes of this study are to constrain the processes involved in the genesis of Cenozoic alkaline basalts in the MMVF and to explore the role of the various mantle reservoirs that contribute to the evolution of the Ross Sea mantle.

2. GEOLOGICAL SETTING AND SAMPLES

The WARS is a Cenozoic extension zone characterized by thin-crust (20–30 km), deep-rift basins within the Ross Sea and Marie Byrd Land (Behrendt, 1999), and significant uplifted roots along the 3500-km-long, 4500-m-high Transantarctic Mountain front (Fig. 1). The uplift of the Transantarctic Mountains was amagmatic and was accompanied by extensional tectonics in the Ross Sea region during the late Cretaceous (Chand et al., 2001; Fitzgerald and Stump, 1997). Since the Eocene, extensive rift-related volcanic activity has affected

the WARS, producing shallow-level intrusions, dike swarms, and volcanoes (Fitzgerald and Stump, 1997; Tonarini et al., 1997; Rocchi et al., 2002).

MMVF basalts in NVL belong to the McMurdo Volcanic Group (Kyle, 1990), a sequence of Cenozoic alkaline igneous rocks that extends at least 800 km from Cape Adare southward to the Ross Ice Shelf, along the western margin of the Ross embayment and the flank of the WARS (Fig. 1). The Cenozoic McMurdo Volcanic Group is divided into Melbourne and Hallett Volcanic Provinces in NVL and Erebus Province in Southern Victoria Land (Kyle et al., 1990). The older intrusive sub-volcanic rocks corresponding to the McMurdo Volcanic Group are known as the Meander Intrusive Group (48–18 Ma, Müller et al., 1991; Tonarini et al., 1997).

The oldest multiple intrusion in Melbourne Province is found at Greene Point and has an age range of 48–39 Ma, dated using the Rb-Sr whole-rock-biotite method (Tonarini et al., 1997; Armienti and Baroni, 1999). The ages of the NVL plutons range from 48 to 23 Ma, and the dikes from 47 to 18 Ma (Tonarini et al., 1997; Rocchi et al., 2002). Thus, the plutonic and sub-volcanic activity in NVL is considered to have overlapped in time during a period 48–18 Ma ago (Rocchi et al., 2002). In contrast, the oldest dated volcanic unit in NVL is 19 Ma (Kyle and Muncy, 1989), and volcanic activity has been continuous to the present day (Rocchi et al., 2002).

The subaerial samples used in this study were collected in the MMVF (Fig. 1), and the submarine samples were dredged in the Terror Rift Region of the Ross Sea during the 2010–2011 research cruise of the *R/V Araon*. Based on spatial distribution, geochemistry, and ages, we separated the sub-aerial samples of the MMVF into two groups (A and B). Four submarine samples selected for analyses had fresh surfaces, which were interpreted as the product of a recent break from dredging.

The MMVF and Terror Rift samples are dark gray or dark in color with sub-aphyric to porphyritic texture and massive or vesicular appearance. Olivine and plagioclase occur as dominant phenocrysts in Group A and B MMVF samples. Clinopyroxene often occurs as microphenocrysts. The groundmass is composed of plagioclase, clinopyroxene, and some Fe-Ti oxide minerals with microcrystalline to cryptocrystalline textures. Olivine occurs as the most prominent phenocrysts in the Terror Rift submarine samples. The olivine phenocrysts are subhedral to euhedral in shape, some partially altered to iddingsite. The groundmass is microcrystalline and consists of plagioclase, clinopyroxene, olivine, and Fe-Ti oxides with basaltic glass.

3. ANALYTICAL METHODS

Ten sub-aerial samples from the MMVF and four dredged submarine basalts from the Terror Rift Region of the Ross Sea, Antarctica, were analyzed to obtain whole-rock major and trace compositions and Sr-Nd-Pb isotope data. Seven

MMVF and three Terror Rift dredged samples were analyzed for K/Ar dating.

Major element abundances were determined on fused glass beads by X-ray fluorescence (XRF) spectrometry using a SHIMADZU XRF-1700 at the Cooperative Laboratory Center, Pukyong National University, Korea, following the method described by Kim et al. (2009). Trace elements were analyzed by inductively coupled plasma mass spectrometry (ICP-MS, Perkin-Elmer, Elan 6100) at the Korea Polar Research Institute (KOPRI). Whole-rock powders (0.1 g) were dissolved in an HF-HNO₃-HClO₄ mixture. The precision was estimated to be within 5% for major elements by XRF and 10% for trace elements by ICP-MS.

Chemical separation and mass spectrometry for Sr, Nd, and Pb isotope analyses were performed at KOPRI. Detailed laboratory procedures of this study closely follow those of Lee et al. (2011). The least altered parts from the representative samples were carefully chosen and crushed to pieces of 1–2 mm in a tungsten-carbide mortar. The pieces were leached in warm 2 N HCl (70 °C) in an ultrasonic bath for 10 min to remove possible contaminants due to sea water alteration, rinsed repeatedly with Milli-Q water, and ground in an agate mortar.

Approximately 50 mg of powdered sample was dissolved in concentrated HF and HClO₄ at 120 °C for 3 days. Pb, Sr, and Nd were all purified from the same solution. Pb was separated from other elements using an anion exchange column with HBr medium and collected in 6 N HCl. After Pb elution, Sr was separated from the solutions by conventional cation column chemistry. Biorad AG50W-X8 (100–200 mesh) was used to separate Sr from the REE as the ion exchange medium. Nd was separated from the bulk REE fraction by second-step cation column chemistry using Ln resin (Eichrom).

Mass spectrometric analysis for Sr, Nd, and Pb isotopes was performed on a thermal ionization mass spectrometer (TIMS, Thermo Finnigan, TRITON) equipped with nine adjustable Faraday cups. Sr and Nd isotopic compositions were measured in static mode with relay matrix rotation (the “virtual amplifier of Finnigan) on a single Ta filament and double Re filaments, respectively. The data were corrected for mass fractionation by normalizing to $^{86}\text{Sr}/^{88}\text{Sr} = 0.1194$ and $^{146}\text{Nd}/^{144}\text{Nd} = 0.7219$ using an exponential law, and all errors were reported as 2σ of the mean. Replicate analyses of NBS 987 and JNdi-1 standards gave $^{87}\text{Sr}/^{86}\text{Sr} = 0.710260 \pm 4$ ($N = 20$, 2σ) and $^{143}\text{Nd}/^{144}\text{Nd} = 0.511847 \pm 1$ ($N = 17$, 2σ).

Pb isotope ratios were determined using the Pb double-spike technique with Southampton-Brest-Lead 207–204 (SBL74) double-spike solution. The SBL74 double-spike solution was originally collaboratively produced and calibrated against NBS 982 ($^{208}\text{Pb}/^{206}\text{Pb} = 1.00016$) by the National Oceanography Center (Southampton, UK), Ifremer (Brest, France), and the former Danish Lithosphere Center (Copenhagen, Denmark). The SBL74 batch used in this analysis was obtained commercially from the University of Southampton, UK. The Pb

isotope data were obtained from two measurements of natural and spiked mixture runs by iterative calculation, adopting an exponential mass-bias correction modified using the power law iteration (Woodhead et al., 1995; Ishizuka et al., 2003). Before Pb was loaded on the single Re filament with silica gel and 0.1 M H₃PO₄, the samples were split into ~100-ng fractions for the natural run and ~10–15-ng fractions for the spiked mixture run, which included adding 2–3 µl of SBL74 (~10–15 ng Pb) to the sample Pb to obtain an optimized ²⁰⁴Pb/²⁰⁶Pb ratio of 0.5–2 in the sample-spike mixture. Replicate analyses of NBS 981 standard gave values of 36.7242 ± 0.0049, 15.4988 ± 0.0016, and 16.9394 ± 0.0016 (mean, 2σ, N = 30) for ²⁰⁸Pb/²⁰⁴Pb, ²⁰⁷Pb/²⁰⁴Pb, and ²⁰⁶Pb/²⁰⁴Pb, respectively. The total averaged blanks were 50 pg for Sr, 30 pg for Nd, and 60 pg for Pb, which were considered negligible relative to the amount of sample analyzed.

For K/Ar age dating, phenocrysts were removed from the samples, and groundmass materials were carefully chosen by hand picking under a binocular microscope. Ar isotopic compositions for K/Ar age determination were measured using a modified VG5400 mass spectrometer (MSIII) in the Geochemical Research Center, Graduate School of Science, University of Tokyo, Japan. K contents for age calculation were from whole-rock major element data obtained by X-ray fluorescence (XRF) spectrometry. The radiogenic ⁴⁰Ar contents of the samples were determined by the unspiked sensitivity method. Analytical procedures and details are described in Nagao et al. (1984), Nagao et al. (1996), and Orihashi et al. (2004).

4. RESULTS

4.1. K/Ar Ages

Table 1 presents 10 new K/Ar ages for the Terror Rift and MMVF samples, together with the age of a standard sample. K/Ar ages for Group A basalts from the MMVF and submarine lavas from the Terror Rift Region of the Ross Sea were determined and agree within the range of analytical errors. The results suggest that Group A and B MMVF and Terror Rift submarine lavas from the study area represent products of three different magmatic episodes. Results for the Group A samples yielded the youngest ages, ranging from 0.1 to 0.3 Ma. The ages for four Group B samples, classified as the oldest group, were identified as 1.25–1.34 Ma. The submarine samples yielded ages of 0.46–0.57 Ma.

4.2. Geochemistry

Table 2 lists major and trace element data for samples collected from the MMVF and Terror Rift Region. The samples are classified as basanite to trachybasalts and plot in the alkaline field in a total alkalis vs. silica classification diagram (Fig. 2). SiO₂ and MgO contents vary from 40.5 to 49.5 wt% and ~3.6 to 9.8 wt%, respectively. Mg numbers (atomic Mg²⁺/100/(Mg²⁺ + Fe²⁺)) range from ~37 to 65. TiO₂ and K₂O contents range from 2.6 to 3.9 wt% and from 0.9 to 2.0 wt%, respectively. The K₂O/Na₂O ratios of the samples are 0.31–0.47, indicating a distinct sodic nature. Overall differentiation trends

Table 1. K-Ar age determination data of Terror Rift submarine and MMVF basalts

Sample	Sampling site		K (wt%)	Weight molten (g)	³⁶ Ar (10 ⁻¹⁰ cm ³ /g)	⁴⁰ Ar/ ³⁶ Ar	Rad. ⁴⁰ Ar (10 ⁻⁸ cm ³ /g)	K-Ar age (Ma)	Air-fraction (%)
	Latitude	Longitude							
TRDR02	76 6.256 S	169 12.675 E	1.65	0.3862	18.23 ± 0.91	307.68 ± 0.69	2.13 ± 0.16	0.33 ± 0.03	96.20
TRDR02	76 6.256 S	169 12.675 E	1.65	0.1148	17.15 ± 0.87	306.83 ± 0.71	1.86 ± 0.15	0.29 ± 0.03	96.47
TRDR03	76 6.256 S	169 12.675 E	1.61	0.3242	22.60 ± 1.13	311.72 ± 0.82	3.55 ± 0.25	0.57 ± 0.05	94.96
TRDR03	76 6.256 S	169 12.675 E	1.61	0.0893	21.53 ± 1.09	309.45 ± 0.66	2.90 ± 0.20	0.46 ± 0.04	95.65
TRDR04	75 57.282 S	165 39.145 E	1.82	0.3519	17.61 ± 0.88	314.27 ± 0.69	3.22 ± 0.20	0.46 ± 0.03	94.19
TRDR04	75 57.282 S	165 39.145 E	1.82	0.1257	17.48 ± 0.88	312.52 ± 0.61	2.89 ± 0.18	0.41 ± 0.03	94.71
MMVFA01	74 13.932 S	164 43.002 E	1.49	0.3578	18.11 ± 0.91	306.48 ± 0.59	1.90 ± 0.14	0.33 ± 0.03	96.58
MMVFA01	74 13.932 S	164 43.002 E	1.49	0.1161	16.27 ± 0.82	305.81 ± 0.71	1.60 ± 0.14	0.28 ± 0.03	96.79
MMVFA04	74 13.917 S	164 44.002 E	1.23	0.3907	7.16 ± 0.36	309.67 ± 0.64	0.98 ± 0.07	0.20 ± 0.01	95.59
MMVFA04	74 13.917 S	164 44.002 E	1.23	0.1561	6.71 ± 0.35	310.57 ± 0.62	0.98 ± 0.07	0.20 ± 0.01	95.31
MMVFA06	74 20.970 S	164 41.423 E	1.43	0.3504	13.09 ± 0.66	299.4 ± 0.58	0.40 ± 0.08	0.07 ± 0.01	98.86
MMVFA06	74 20.970 S	164 41.423 E	1.43	0.1247	12.99 ± 0.66	301.08 ± 0.66	0.66 ± 0.09	0.12 ± 0.02	98.31
MMVFB01	74 29.195 S	165 17.383 E	1.65	0.3424	4.00 ± 0.20	496.68 ± 2.21	8.03 ± 0.42	1.25 ± 0.09	59.60
MMVFB02	74 29.195 S	165 17.383 E	1.61	0.4124	8.28 ± 0.42	397.04 ± 0.95	8.36 ± 0.43	1.34 ± 0.07	74.55
MMVFB03	74 29.195 S	165 17.383 E	1.64	0.3059	10.21 ± 0.52	377.89 ± 1.10	8.36 ± 0.43	1.31 ± 0.09	78.33
MMVFB04	74 29.195 S	165 17.382 E	1.66	0.362	7.96 ± 0.40	403.37 ± 1.47	8.54 ± 0.44	1.32 ± 0.07	73.38
Standard sample									
Baba tuff #c			6.56	0.0293	15.55 ± 0.89	2219.65 ± 61.5	299.08 ± 15.3	11.71 ± 0.64	13.34
Baba tuff #120304a			6.56	0.0273	13.58 ± 0.82	2529.92 ± 87.8	303.47 ± 15.6	11.88 ± 0.65	11.70

Table 2. Major and trace element compositions of Terror Rift submarine and MMVF basalts

Sample Age (Ma)	TRDR01 0.333	TRDR02 0.568	TRDR03 0.455	TRDR04 0.278	MMVFA01 0.278	MMVFA02	MMVFA03	MMVFA04 0.205	MMVFA05	MMVFA06 0.119	MELB01 1.253	MMVFB02 1.338	MMVFB03 1.312	MMVFB04 1.325
Major elements (wt%)														
SiO ₂	40.51	42.39	42.11	43.74	47.00	46.79	46.39	46.38	44.71	49.14	49.99	49.35	47.53	47.66
Al ₂ O ₃	12.58	14.28	13.93	13.19	14.46	15.73	13.97	15.85	14.72	15.52	14.67	14.72	15.15	15.09
TiO ₂	2.65	2.93	2.83	3.95	2.90	2.87	2.84	3.24	3.33	3.38	2.61	2.65	2.76	2.76
Fe ₂ O ₃	12.45	12.41	12.44	14.16	15.31	12.58	14.59	13.70	13.86	12.40	14.27	14.54	14.75	15.10
MnO	0.20	0.17	0.19	0.20	0.27	0.19	0.25	0.21	0.18	0.18	0.23	0.23	0.23	0.24
MgO	9.81	7.17	7.68	8.28	4.04	5.50	4.47	4.98	7.22	4.34	3.58	3.72	3.81	3.87
CaO	9.87	11.88	11.89	11.70	7.93	8.83	8.79	9.30	10.64	8.96	6.89	7.08	7.49	7.38
Na ₂ O	3.89	4.97	4.75	2.74	4.33	3.91	3.64	3.75	3.18	3.89	4.40	4.24	4.39	4.54
K ₂ O	1.83	1.98	1.94	0.96	1.79	1.52	1.70	1.49	1.00	1.72	1.99	1.94	1.98	2.00
P ₂ O ₅	0.82	0.96	0.91	0.57	1.63	0.83	1.50	1.31	0.89	0.76	1.56	1.62	1.67	1.75
LOI ^a	4.89	0.55	1.09	0.51	0.19	1.67	1.67	0.00	0.14	0.00	0.00	0.00	0.00	0.00
K ₂ O/Na ₂ O	0.47	0.40	0.41	0.35	0.41	0.39	0.47	0.40	0.31	0.44	0.45	0.46	0.45	0.44
Mg# ^b	64.73	57.37	58.98	57.68	38.06	50.44	41.67	45.87	54.85	44.91	36.92	37.34	37.55	37.39
Trace elements (ppm)														
Li	9.4	6.9	6.5	5.6	7.5	5.7	7.0	5.4	4.5	7.9	8.4	8.2	7.5	8.7
Rb	38.1	48.4	49.0	26.0	29.5	33.3	31.5	22.5	18.6	45.2	35.9	33.7	40.4	38.5
Sr	818	999	932	671	875	905	896	874	764	680	884	824	843	866
Y	27.2	31.5	29.2	23.0	37.9	22.6	25.7	29.2	23.6	30.5	30.7	42.3	24.4	48.8
Zr	224	266	259	237	251	292	261	195	169	258	369	318	346	349
Nb	91.4	107.9	105.2	56.4	71.0	77.3	69.6	52	44.3	63.1	80.0	76.7	75.6	82.6
Cs	0.5	0.7	0.8	0.4	0.3	0.4	0.5	0.1	0.2	0.7	0.2	0.3	0.8	0.4
Ba	618	767	800	309	823	494	865	693	397	503	692	633	702	690
La	62.3	77.8	68.2	43.5	66.4	43.5	44.1	46.5	33.3	44.7	41.6	65.0	36.2	72.8
Ce	114.6	143.5	125.3	90.7	138.3	89.2	93.5	97.5	70.3	92.4	92.0	140.3	76.8	154.1
Pr	12.9	15.7	14.1	10.8	17.1	10.6	11.5	12.3	8.8	11.1	11.7	17.2	9.6	19.2
Nd	47.9	59.8	54.5	43.1	70.7	41.9	48.2	52.0	37.8	44.8	48.9	72.5	39.5	80.0
Sm	9.0	11.1	10.0	8.4	13.8	7.7	9.3	10.2	7.6	9.1	9.9	14.4	7.8	16.1
Eu	2.7	3.4	3.1	2.6	5.7	2.9	4.4	4.2	3.0	3.0	4.0	4.8	3.3	5.2
Gd	7.8	9.5	9.3	7.3	12.1	6.9	8.5	9.2	7.1	8.4	8.9	12.9	6.9	14.2
Tb	1.1	1.2	1.2	1.0	1.6	1.0	1.1	1.2	1.0	1.2	1.2	1.8	1.0	1.9
Dy	5.9	6.8	6.8	5.3	8.5	5.1	5.9	6.6	5.4	6.7	6.7	9.7	5.5	10.5
Ho	1.1	1.2	1.2	0.9	1.5	0.9	1.0	1.2	1.0	1.2	1.2	1.7	1.0	1.9
Er	2.9	3.3	3.1	2.4	3.9	2.4	2.7	3.0	2.5	3.3	3.2	4.4	2.7	4.9
Tm	0.4	0.4	0.4	0.3	0.5	0.3	0.3	0.4	0.3	0.4	0.4	0.6	0.4	0.6
Yb	2.3	2.7	2.6	1.9	2.9	2.0	2.2	2.3	1.8	2.6	2.8	3.4	2.5	3.8
Lu	0.3	0.4	0.4	0.3	0.4	0.3	0.6	0.3	0.3	0.4	0.4	0.5	0.4	0.5
Hf	5.2	6.0	5.9	5.9	6.1	6.8	6.0	4.9	4.2	6.3	8.2	7.6	8.0	8.0
Ta	5.8	6.7	6.4	3.9	4.7	4.9	4.3	3.7	3.1	4.5	4.3	4.9	4.0	5.2
W	2.0	2.3	6.5	4.1	1.1	1.6	1.1	0.8	1.3	4.6	2.4	1.1	3.0	3.3
Pb	3.4	3.8	3.9	3.5	3.4	2.5	3.0	2.6	2.3	4.7	2.9	3.5	4.6	4.5
Th	8.5	9.8	9.3	6.5	5.9	5.6	4.2	4.6	3.3	7.3	4.9	6.0	4.6	6.5
U	2.2	2.4	2.3	1.4	1.4	1.5	1.0	1.0	0.9	1.8	1.1	1.3	1.1	1.7
Ni	121	70	81	135	3	55	3	29	79	24	5	5	5	6

^aL.O.I = loss on ignition.^bMg# = 100Mg/(Mg + Fe²⁺), assuming Fe₂O₃/FeO = 0.15.

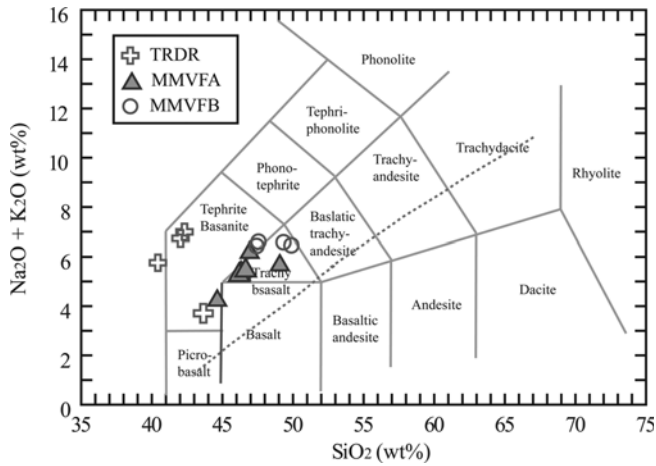


Fig. 2. Total alkalis vs. SiO₂ diagram for Terror Rift submarine and MMVF basalts (the framework is after Le Bas et al., 1985). Abbreviations: TRDR, Terror Rift Dredge basalts; MMVFA and MMVFB, Mt. Melbourne Volcanic Field Group A and B basalts.

show a general increase in SiO₂, Al₂O₃, Fe₂O₃^T, Na₂O, K₂O, and P₂O₅ with decreasing MgO (Fig. 3), indicating a significant role of olivine + pyroxene fractionation. Generally, submarine Terror Rift lavas have higher MgO (9.8–7.2 wt%) and CaO (11.9–9.9 wt%) and lower SiO₂ (40.5–43.7 wt%) and Al₂O₃ (12.6–14.3 wt%) contents than Group A and B samples from the MMVF, and they show distinct variation in the differentiation trend.

Trace elemental abundances normalized to primitive mantle for the Terror Rift submarine and MMVF samples were compared to previous data for basaltic rocks of the McMurdo Volcanic Group. The compositions of the MMVF and Terror Rift samples plot within the range of previously published data (Fig. 4). Overall variations display typical OIB-like patterns, but slightly higher concentrations of all incompatible elements compared with an average OIB. They are also characterized by a prominent depletion in K, Pb, and Ti and enrichment in Nb and Ta relative to other highly incompat-

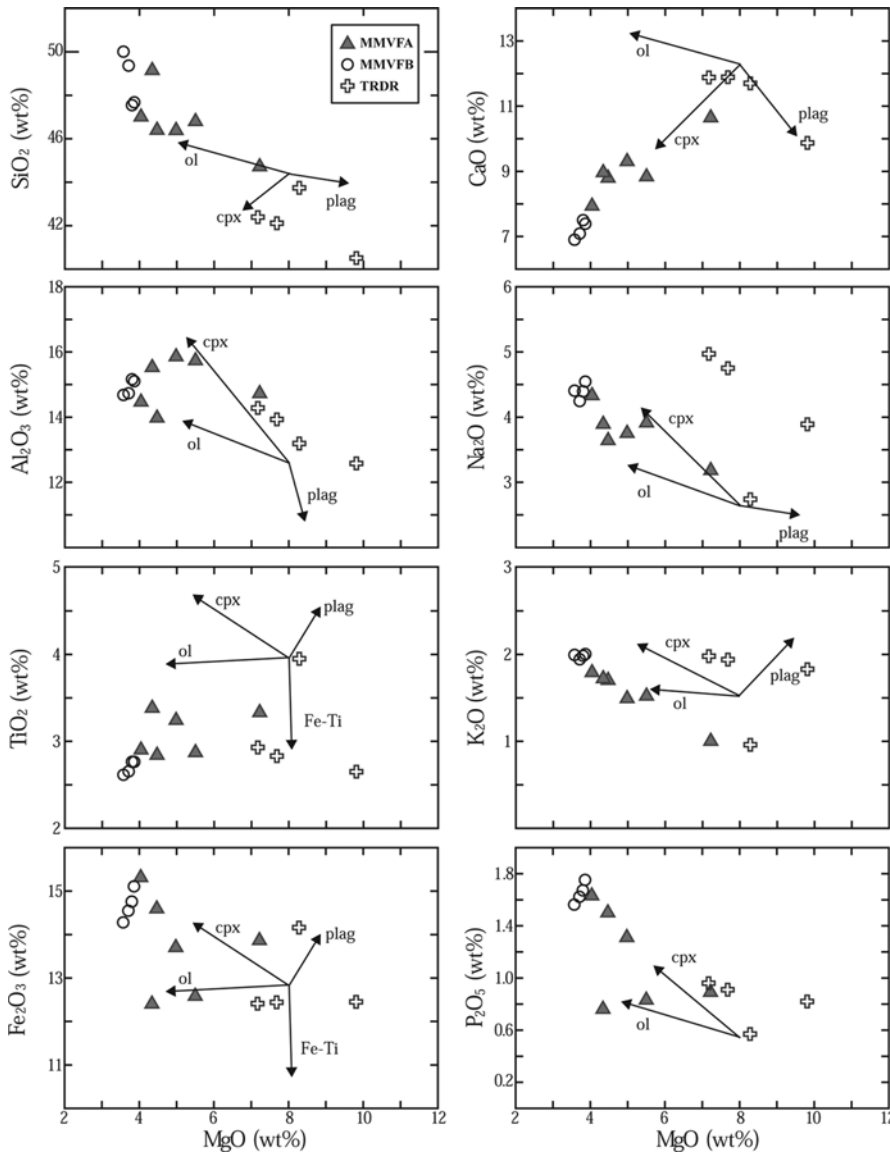


Fig. 3. Major element variation diagrams (wt%) for Terror Rift submarine and MMVF basalts. Fractional crystallization vectors are shown. Abbreviations: cpx, clinopyroxene; ol, olivine; plag, plagioclase; Fe-Ti, Fe-Ti oxide minerals.

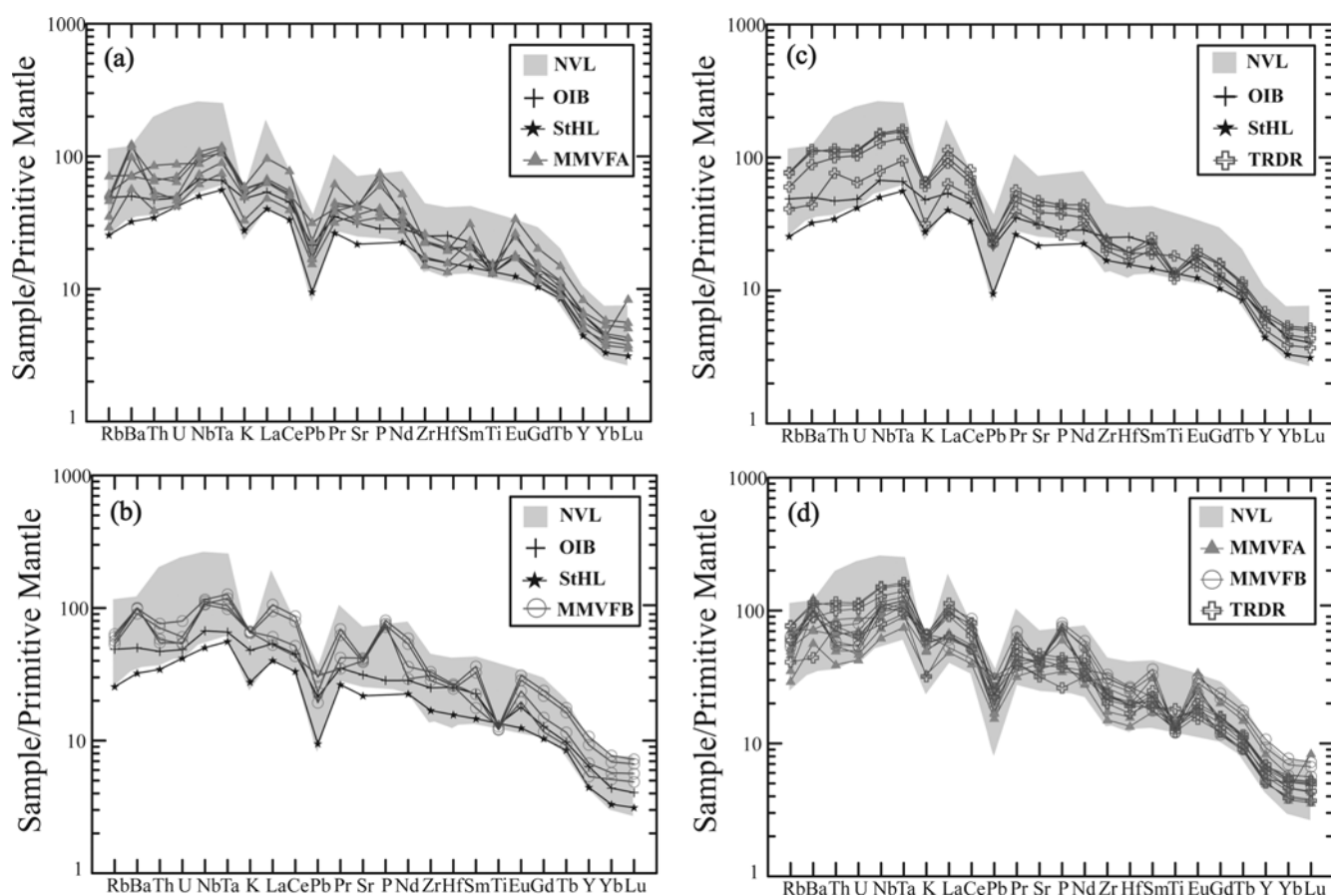


Fig. 4. Trace-element patterns normalized to primitive mantle (McDonough and Sun, 1995) for Terror Rift submarine and MMVF basalts. Patterns of the studied samples and average OIB are compared with those of McMurdo Volcanic Group basalts from NVL and St. Helena HIMU-OIB. Data sources for comparison are average OIB, McDonough and Sun (1995); NVL, Nardini et al. (2009); St. Helena, PETDB database (<http://www.petdb.org/index.jsp>).

ible elements.

The Nb, Ta, and LREE (Light Rare Earth element) enrichment are most pronounced in Terror Rift submarine samples with a much steeper overall REE slope [(La/Yb)_n = 16.3–21.1, Fig. 4]. Group A and B samples from the MMVF show similar incompatible element abundances, but Group B samples display somewhat flatter REE patterns [Group A, (La/Yb)_n = 12.2–16.6; Group B, (La/Yb)_n = 10.3–13.8], possibly suggesting higher degrees of partial melting. Slightly positive Eu anomalies are shown by Group A and B basalts from the MMVF, but there is no evidence of cumulus plagioclase. All three groups of basaltic samples display steep HREE (Heavy Rare Earth Element) patterns (e.g., (Sm/Yb)_N and (Dy/Yb)_N > 1), indicating the presence of residual garnet in the magma source.

The Sr, Nd, and Pb isotopic compositions of the studied samples are shown in Figure 5 with data from previous studies on Melbourne Volcanic group rocks. They display a range of values for ⁸⁷Sr/⁸⁶Sr (0.70299–0.70398), ¹⁴³Nd/¹⁴⁴Nd (0.51284–0.51297), and ²⁰⁶Pb/²⁰⁴Pb (18.6059–19.683) (Table 3). They display a considerably higher range of ²⁰⁶Pb/²⁰⁴Pb, in contrast to the limited compositional variations in ⁸⁷Sr/⁸⁶Sr and ¹⁴³Nd/¹⁴⁴Nd. Submarine lavas dredged from the Terror Rift Region have

slightly higher ratios of ²⁰⁶Pb/²⁰⁴Pb (19.373–19.565) and ¹⁴³Nd/¹⁴⁴Nd (0.51290–0.51297) and less radiogenic ⁸⁷Sr/⁸⁶Sr (0.70300–0.70340), forming fields distinct from those of the Group A and B samples (Fig. 5). The Terror Rift submarine samples show compositions tending toward HIMU-OIBs, whereas compositions of Group A and B MMVF samples tend toward an enriched mantle-type end-member (EMI) (Fig. 5).

5. DISCUSSION

5.1. Geochemical Constraints and Melting Regime

The MMVF basalts and Terror Rift submarine lavas contain variable proportions of olivine, clinopyroxene, and plagioclase phenocrysts. Close correlations between MgO and SiO₂ and between CaO/Al₂O₃ and MgO suggest fractional crystallization of olivine and clinopyroxene. In contrast, significant fractionation of plagioclase cannot be assumed due to the lack of negative Eu anomalies. The fractionation of olivine and clinopyroxene can affect the abundances of some major and trace elements, such as SiO₂, MgO, Fe₂O₃, CaO, Ni, and Cr. However, fractional crystallization of these phases cannot

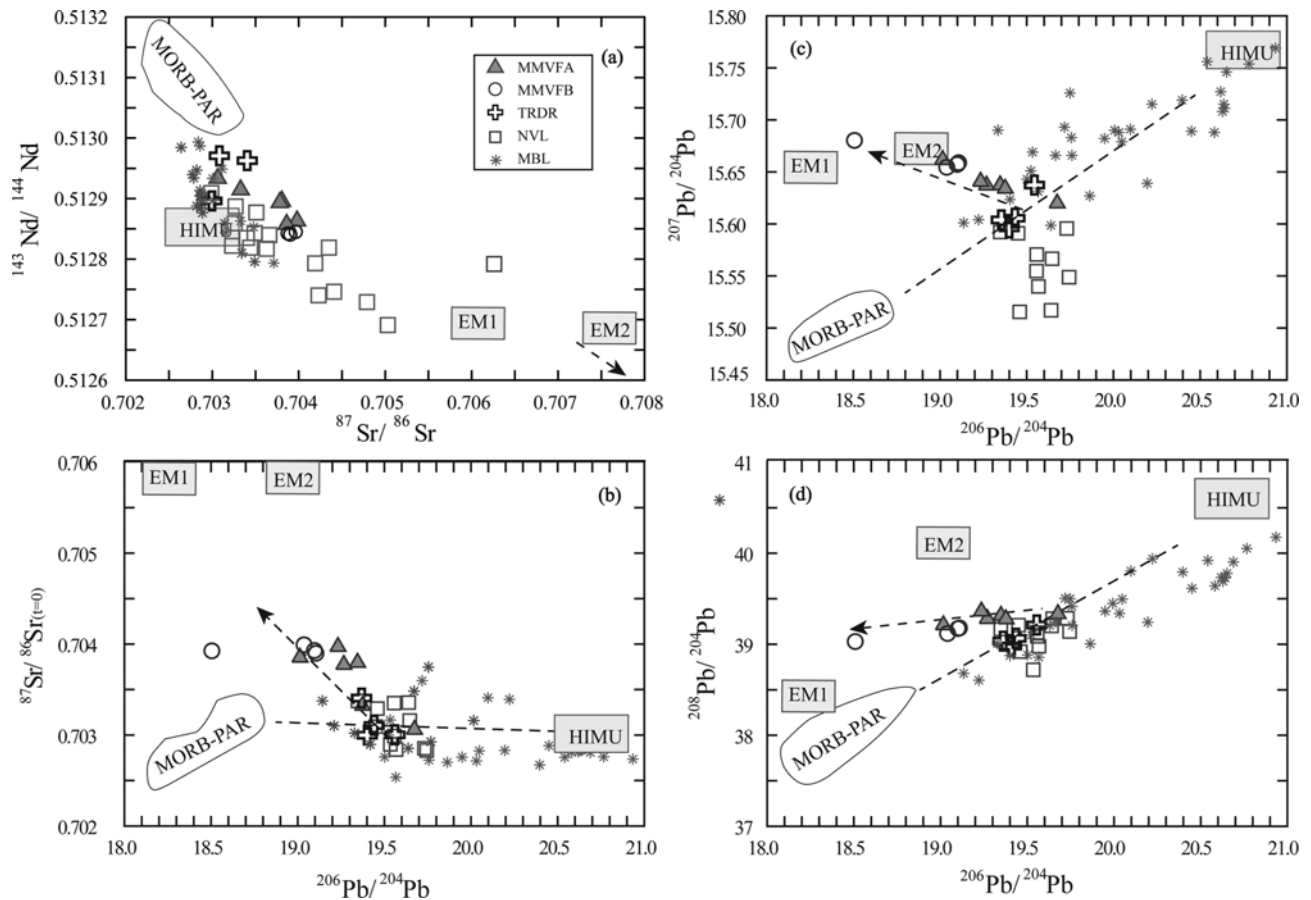


Fig. 5. Sr-Nd-Pb isotopic compositions of Terror Rift submarine and MMVF basalts. Data for McMurdo Volcanic Group basalts from Northern Victoria Land (NVL, Nardini et al., 2009) and Marie Bird Land basalts (MBL, Panter et al., 2006; Hart et al., 1997) are displayed together for comparison. MORB-PAR (Pacific Antarctic Ridge) data are from Vlastlic et al. (2000). End-member mantle components are from Zindler and Hart (1986).

Table 3. Sr, Nd and Pb (double-spike corrected) isotopic compositions of Terror Rift submarine and MMVF basalts

	Sample name	$^{87}\text{Sr}/^{86}\text{Sr}$	2 s.e.	$^{143}\text{Nd}/^{144}\text{Nd}$	2 s.e.	ϵ_{Nd}^a	$^{206}\text{Pb}/^{204}\text{Pb}$	2 s.e.	$^{207}\text{Pb}/^{204}\text{Pb}$	2 s.e.	$^{208}\text{Pb}/^{204}\text{Pb}$	2 s.e.
Dredge	TRDR01	0.703405	8	0.512963	6	6.3	19.3734	11	15.6036	10	39.0068	31
	TRDR02	0.703082	9	0.512971	6	6.5	19.4344	7	15.6013	7	39.0203	20
	TRDR03	0.702998	10	0.512963	6	6.3	19.4108	6	15.5984	5	38.9991	17
	TRDR04	0.702996	6	0.512896	4	5.0	19.5653	7	15.6362	6	39.1856	20
Mt. Melbourne A	MMVFA01	0.703805	10	0.512896	4	5.0	19.3532	16	15.6398	15	39.3240	47
	MMVFA02	0.703062	16	0.512933	4	5.8	19.6829	13	15.6222	12	39.3436	37
	MMVFA03	0.703781	6	0.512893	4	5.0	19.2740	10	15.6396	9	39.2885	28
	MMVFA04	0.703980	7	0.512863	4	4.4	19.2400	29	15.6432	27	39.3711	84
	MMVFA05	0.703328	6	0.512914	5	5.4	19.3819	15	15.6365	14	39.2853	44
	MMVFA06	0.703861	16	0.512857	5	4.3	19.0198	10	15.6644	10	39.2192	30
Mt. Melbourne B	MMVFB01	0.703883	10	0.512841	4	4.0	19.1124	11	15.6593	10	39.1625	31
	MMVFB02	0.703913	8	0.512839	4	3.9	19.1040	9	15.6577	9	39.1561	27
	MMVFB03	0.703977	9	0.512843	3	4.0	19.0438	11	15.6549	10	39.1008	32
	MMVFB04	0.703910	5	0.512839	3	3.9	18.5096	14	15.6809	13	39.0118	41

^a ϵ_{Nd} values were calculated using $\epsilon_{\text{Nd}} = [(^{143}\text{Nd}/^{144}\text{Nd})_{\text{sample}} / (^{143}\text{Nd}/^{144}\text{Nd})_{\text{CHUR}} - 1] \times 10^4$, where $(^{143}\text{Nd}/^{144}\text{Nd})_{\text{CHUR}} = 0.512638$.

account for the variations in highly incompatible trace elements and Sr-Nd-Pb isotopic compositions. Moreover, the

Ce/Pb and Nb/U ratios of the MMVF and Terror Rift samples (Ce/Pb = 25–35 and Nb/U = 45–60) are significantly

higher than values for the continental crust ($Ce/Pb = 10$ and $Nb/U = 4$, Hofmann et al., 1986) and are within the range of oceanic basalts, suggesting an insignificant role of crustal contamination in the magma generation. The Ce/Pb and Nb/U ratios are commonly used as a key proxy to trace the effect of crustal contamination in continental alkali basalts because of their constant and higher values in oceanic basalts ($Ce/Pb = 25 \pm 5$, and $Nb/U = 47 \pm 7$; Hofmann et al., 1986) compared with those in continental crust or island arc basalts (Taylor and McLennan, 1985). These various lines of evidence suggest that the incompatible trace element ratios and Sr-Nd-Pb isotopic compositions of the MMVF and Terror Rift basalts reflect the primary nature of mantle sources contributing to the magma generation.

The Terror Rift submarine samples show distinct compositional variations having 1) lower SiO_2 and Al_2O_3 and higher MgO and CaO contents compared with the subaerial MMVF samples, 2) higher ratios of more to less incompatible elements (e.g., La/Yb , La/Sm , Nb/Y , Th/Yb , and U/Pb), and 3) higher $^{206}Pb/^{204}Pb$ and $^{143}Nd/^{144}Nd$, and lower $^{87}Sr/^{86}Sr$ isotopic compositions. These distinct geochemical differences between the Terror Rift submarine and MMVF sub-aerial samples imply that the magma genesis took place under different physico-chemical conditions; they cannot be explained simply by varying degrees of partial melting of a homogeneous source, but reflect the different contribution of various mantle sources.

To aid evaluation of the source characteristics and melting processes of the MMVF and Terror Rift basalts, we compared the incompatible element ratios to those of representative HIMU-type OIBs and global averages of alkali basalts (Fig.

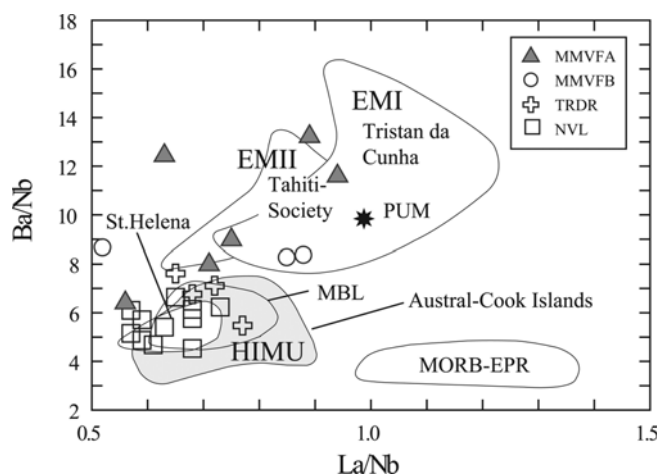


Fig. 6. Ba/Nb vs. La/Nb ratios. Data sources for NVL and MBL samples are the same as in Figure 5. Data for Austral-Cook Island, St. Helena basalts, which are representative HIMU-OIBs, Tristan da Cunha (EMI), and Tahiti-Society (EMII) are compiled from the PETDB database (<http://www.petdb.org/index.jsp>). MORB-EPR (East Pacific Rise) data are from the PETDB database (<http://petdb.org/index.jpg>). PMU, Primitive Upper Mantle from McDonough and Sun, 1995.

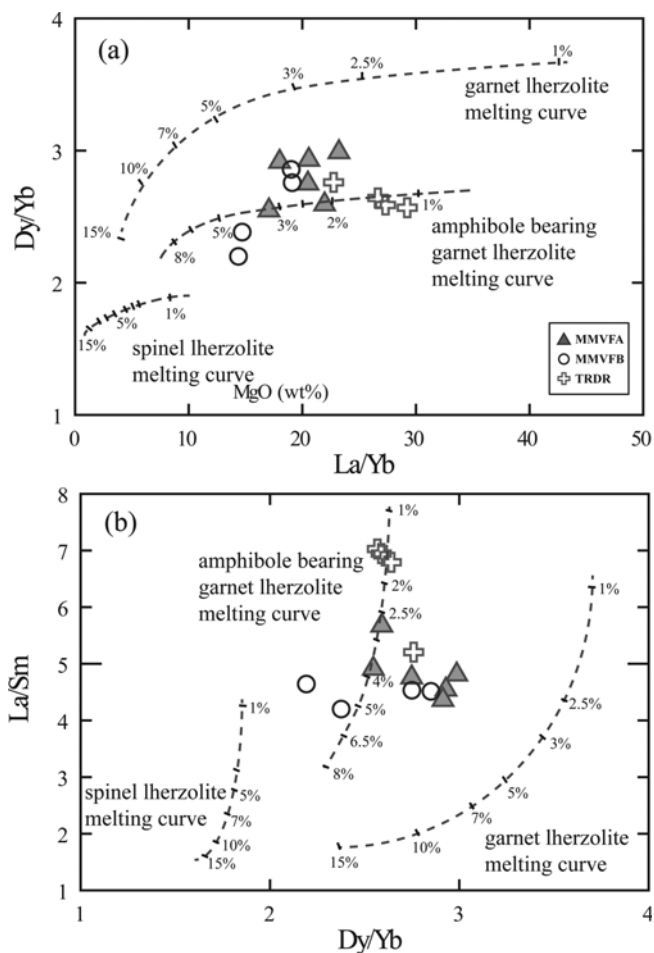


Fig. 7. Calculated partial melting curves assuming non-modal batch melting of spinel, garnet and amphibole-bearing garnet lherzolite. Phase proportions in solid and melt modes for a hypothetical spinel lherzolite used for model calculations are $ol_{0.578} + opx_{0.27} + cpx_{0.119} + sp_{0.033}$ and $ol_{0.1} + opx_{0.27} + cpx_{0.5} + sp_{0.13}$, and for a hypothetical garnet lherzolite $ol_{0.598} + opx_{0.211} + cpx_{0.115} + gt_{0.115}$ and $ol_{0.05} + opx_{0.20} + cpx_{0.30} + gt_{0.45}$, respectively. Phase proportions in solid and melt modes for a hypothetical amphibole-bearing garnet lherzolite are $ol_{0.514} + opx_{0.213} + cpx_{0.123} + gt_{0.075} + amp_{0.075}$ and $ol_{0.05} + opx_{0.18} + cpx_{0.205} + gt_{0.25} + amp_{0.315}$, respectively.

6), and we performed REE modeling of the estimated mantle peridotite sources (Fig. 7). The low LILE/Nb (Large-ion lithophile elements/Nb) values of the Terror Rift submarine lavas are comparable to those of other continental basalts related to the WARS and are especially similar to those of HIMU-type OIBs (St. Helena and the Austral-Cook Island chain). In contrast, the LILE/Nb ratios of the MMVF Group A and B basalts are higher than those of the other continental alkali basalts from the WARS, indicating contributions of more enriched mantle components to the magma generation.

Figure 7 presents the results of partial melting models developed with spinel and garnet lherzolite sources of different residual mineral assemblages. These models used the non-modal batch melting equations of Shaw (1970), with the K_D

Table 4. Mantle source compositions (S1, S2) and mineral/melt partition coefficients (D -values) used in calculations for Figure 7

	Spinel lherzolite S1 (ppm)	Garnet lherzolite S1	Amphibole garnet lherzolite S2	$D^{ol/melt}$	$D^{opx/melt}$	$D^{cpx/melt}$	$D^{sp/melt}$	$D^{gt/melt}$	$D^{amp/melt}$
La	0.8931	0.8931	1.58	0.0004	0.002	0.054	0.01	0.01	0.17
Sm	0.5772	0.5772	0.83	0.0013	0.01	0.26	0.01	0.217	0.76
Dy	0.9581	0.9581	1.14	0.0017	0.022	0.33	0.01	1.06	0.78
Yb	0.6409	0.6409	0.81	0.0015	0.049	0.28	0.01	4.03	0.59

S1 source concentrations are from Tang et al. (2006) and S2 are from McCoy-west et al. (2010).

Modelling used the distribution coefficients of McKenzie and O'Nions (1991) for ol, opx, cpx and sp, and those for amp from Chazot et al. (2006).

Abbreviations: ol, olivine; opx, orthopyroxene; cpx, clinopyroxene; sp, spinel; gt, garnet; amp, amphibole.

values of McKenzie and O'Nions (1991) and Chazot et al. (1996). Potential mantle sources for the spinel and garnet lherzolite were taken from McDonough and Sun (1995). Mantle source compositions and K_D values used in REE modeling are listed in Table 4. The modal mineralogy and melting proportions of the source mantle rocks used in the model calculations were similar to those used in other partial melting calculations (e.g., McCoy-West et al., 2010; Choo et al., 2012). The amphibole-bearing garnet lherzolite mantle source was assumed to be a moderately enriched HIMU mantle source comparable to that of McCoy-West et al. (2010).

Partial-melting modeling showed that the calculated Dy/Yb ratio for the melting of a garnet lherzolite source was too high compared with that of the Terror Rift and MMVF samples, suggesting the presence of a phase that has a greater partition coefficient for MREE than HREE, such as amphibole in mantle sources (amphibole: $D_{Dy} = 0.78$, $D_{Yb} = 0.59$, in garnet lherzolite source, Chazot et al., 1996). Modeling an amphibole-bearing garnet lherzolite source produced a closer fit to the compositions of the Terror Rift samples in the Dy/Yb vs. La/Yb and La/Sm vs. Dy/Yb plots. The data for the Terror Rift samples are consistent with 1–2% melting of an amphibole-bearing garnet lherzolite source. In contrast, the REE data of the MMVF Group A and B samples could not be modeled satisfactorily with either spinel and garnet lherzolite or amphibole-bearing garnet lherzolite sources. The MMVF Group A and B samples generally show large variations in MREE composition, reflecting the heterogeneous characteristics of their source; it is assumed that the modal proportions of amphibole in their mantle sources and source compositions are quite different from the source of the Terror Rift submarine lavas. Although the results of the model calculations of estimated peridotite source rocks do not display a close fit with the data of the MMVF basalts, the degree of partial melting of the MMVF Group A and B samples appears to be greater (about 2–5%) than that of the Terror Rift submarine samples (about 1–2%).

Numerous previous researchers have proposed that the WARS-related Cenozoic intraplate basalts likely originated from the amphibole-bearing metasomatized lithospheric mantle, which had been progressively modified by asthenosphere-derived melt (e.g., Panter et al., 2006; Nardini et al., 2009;

McCoy-West et al., 2010). Negative K anomalies in a primitive mantle-normalized trace element abundance plot, commonly observed throughout Cenozoic intraplate basalts in NVL and Marie Byrd Land (e.g., Hart et al., 1997; Panter et al., 2000, 2006; Nardini et al., 2009), West Antarctica, have been considered as crucial evidence for the presence of amphibole or phlogopite, which are assumed to retain alkali elements such as K, Rb, and Ba during partial melting in the mantle source. Melts with phlogopite in equilibrium are expected to have higher Rb/Sr (>0.1) and lower Ba/Rb (<20) ratios compared with melts from an amphibole-bearing source (Rb/Sr < 0.06, Ba/Rb > 20) because of the different incompatibility in Rb and Ba of phlogopite and amphibole (Furman and Graham, 1999). Rb/Sr and Ba/Rb ratios of the Terror Rift and MMVF basalts are 0.02–0.06 and 11.9–30.8, respectively, suggesting the presence of amphibole rather than phlogopite as the K-bearing phase in their mantle sources. The ubiquitous presence of metasomatic vein material, including secondary amphiboles produced by metasomatic reaction, in mantle-peridotite xenoliths (Coltorti et al., 2004; Perinelli et al., 2006; Melchiorre et al., 2011) recovered from the NVL volcanic lavas provides additional support for the presence of residual amphibole in the mantle source region.

The presence of residual amphibole in the source of the MMVF and Terror Rift basalts provides limits for the estimation of the melting depths of magma generation. Experimental studies show that amphiboles are stable at high temperatures (~1300 °C, McKenzie and Bickle, 1988) and high pressures (up to 3–5 GPa, Foley, 1991; Trønnes, 2002), depending on their composition. However, at these high pressures, amphiboles are stable only in the cold and deep continental lithospheric mantle, not in the convecting asthenospheric mantle (Class and Goldstein, 1997). This suggests that the contribution of a lithospheric mantle source should be considered in the petrogenetic interpretation of MMVF and Terror Rift magma generation.

5.2. HIMU- and EM-like Components

The trace element variation and Sr-Nd-Pb isotope data of the MMVF and Terror Rift submarine lavas suggest that various mantle sources, such as enriched mantle and depleted

MORB (Mid-oceanic Ridge Basalt)-like (i.e., depleted mantle; DM) and HIMU-like components were incorporated into the magma genesis. The obvious geochemical distinction between the MMVF and Terror Rift basalts reflects differences in their respective mantle sources and melting processes. The isotope data of the Terror Rift samples lie along the binary mixing line between the DM (Pacific-Antarctic Ridge [PAR]-MORB) and HIMU-like components in plots of $^{87}\text{Sr}/^{86}\text{Sr}$ and $^{143}\text{Nd}/^{144}\text{Nd}$ vs. $^{206}\text{Pb}/^{204}\text{Pb}$ (Fig. 5). In contrast, the data of the MMVF Group A and B samples fall in a triangle defined by a depleted MORB mantle, a HIMU-like component, and an enriched component. An EMI-like source component appears to have been added to a mixture of depleted MORB and HIMU-like components. Regardless of differences in the relative contribution of a HIMU-like component to the genesis of the MMVF and Terror Rift samples, the Pb isotopic compositions clearly show a HIMU source.

This latter feature appears to be common in volcanics throughout Antarctica (Marie Byrd Land and Victoria Land), as well in Zealandia and eastern Australia. It has been argued that the volcanic features of these regions collectively constitute a large Mesozoic to Cenozoic diffuse alkaline magmatic province (DAMP; Finn et al., 2005). The nature of the origin of the extremely broad distribution (>5000 km) and significant persistence (~100 Ma) of HIMU-type alkaline volcanism throughout the DAMP has been a topic of significant debate for several decades (e.g., Hart et al., 1997; Finn et al., 2005; Panter et al., 2006; Timm et al., 2010).

DAMP encompasses eastern Australia, Zealandia, several sub-Antarctic islands, and West Antarctica. All of these regions were contiguous prior to the breakup of Gondwanaland (~100 Ma), suggesting that the HIMU-like signature has a common origin, most likely a lithospheric source (Hart et al., 1997; Panter et al., 2000). Various hypotheses have been proposed for the HIMU signature of the DAMP, involving derivation from a fossil HIMU plume head that invaded the lithosphere before the breakup of Gondwanaland (Rocholl et al., 1995; Hart et al., 1997; Panter et al., 2000) or the metasomatization of continental lithosphere by plume- or subduction-related fluids (Cook et al., 2005; Panter et al., 2006; Sprung et al., 2007). Alternatively, delamination of lithospheric mantle fertilized by plume- or subduction-related magmas and incorporation into asthenosphere undergoing decompression melting has also been suggested (Hoernle et al., 2006; Timm et al., 2009, 2010).

The HIMU signature of the DAMP magmatism in all these hypotheses, regardless of whether the origin was lithospheric or asthenospheric, is attributed to fertilization of proto-lithospheric mantle by plume or metasomatizing fluids. Previous geochemical and petrological studies of mantle xenoliths from various localities of NVL provide crucial evidence for the presence of the HIMU signature in the subcontinental lithospheric mantle (Coltorti et al., 2004; Perinelli et al., 2006; Melchiorre et al., 2011). These investigations have shown

that the lithospheric mantle beneath the WARS is chemically and mineralogically highly heterogeneous, which provides additional evidence to support the hypothesis of partial melting and metasomatic processes resulting in HIMU-type metasomatized sources (Coltorti et al., 2004; Perinelli et al., 2006; Melchiorre et al., 2011). In summary, the widespread HIMU-like mantle component persisting over ~100 Ma in the volcanism of the DAMP is thought to be related to the presence of metasomatized Gondwanaland proto-lithospheric mantle in the source region.

The enriched geochemical signal of alkaline lavas erupted in oceanic island and continental settings is thought to be closely related to subduction and recycling of oceanic plates together with small amounts of lower and upper continental crust (Willbold and Stracke 2010; Stracke, 2012). Subduction throughout the Mesozoic along the Gondwana margin could have overprinted the WARS lithospheric mantle with an EM-type mantle component. A number of studies on peridotite and pyroxenite xenoliths from NVL alkali lavas have proposed that metasomatic veins produced by infiltration of subduction-related fluids or hydrous low-degree melts from recycled oceanic crust or lower crustal component, not only with HIMU-type but also with EM-type geochemical signatures, are ubiquitous elsewhere in the dispersed Gondwana super-continental lithospheric mantle (Becker, 1996; Coltorti et al., 2004; Perinelli et al., 2006; Melchiorre et al., 2011; Martin et al., 2013).

5.3. Magma Generation

Recently, a number of studies (Rocchi et al., 2005; Storti et al., 2007; Nardini et al., 2009; Perinelli et al., 2011) have proposed that the development of the Ross Sea Rift System and the associated Cenozoic magmatic activity in NVL are closely related to dextral transtensional movements connected with plate kinematic adjustments in the Southern Hemisphere rather than to an active mantle plume. Continuous volcanism in restricted areas over long time periods and a lack of progression in volcanic age relative to plate motion (Rocholl et al., 1995; Rocchi et al., 2002) provide constraints indicating that the Ross Sea Cenozoic magmatism was not related to plume activity (Panter et al., 2006; Perinelli et al., 2011). Petrogenetic models based on the petrology and geochemistry of the volcanic rocks in NVL assume interaction between melting of lithospheric mantle, including veins of subduction or fossil "HIMU-like" components, and decompression melting of upwelling asthenosphere (Panter et al., 2006; Nardini et al., 2009; Perinelli et al., 2011). The proportions of lithospheric and asthenospheric sources depend on various physicochemical parameters, such as lithospheric thickness, extension rate and heat flow (e.g., Gallagher and Hawkesworth 1992; Hawkesworth and Gallagher 1993; Sprung et al., 2007), which are reflected in variations in magma composition.

Several models have been applied to study of the heat

source of the NVL magma generation in a non-plume-related tectonic setting. Armienti and Perinelli (2010) and Perinelli et al. (2011) proposed that edge-driven convective mantle flow caused by lateral temperature and viscosity contrasts at the boundary between the thick East Antarctic Craton and the thinned crust of Ross Sea provided the heat source for magma generation.

Lithospheric delamination/detachment that caused gravitational or Rayleigh-Taylor instabilities has been suggested as an alternative mechanism for asthenospheric upwelling in the Gondwana continental margin (Hoernle et al., 2006; Timm et al., 2009, 2010). Modeling of delamination/detachment of lithospheric mantle requires a lower lithospheric mantle that is cooler and denser than its surroundings to generate gravitational or Rayleigh-Taylor instabilities (Schott et al., 2000; Elkins-Tanton, 2007). Generally, gravitational instabilities can be produced through crustal thickening during the convergent tectonic regime (e.g., Schott and Schmeling, 1998; Schott et al., 2000; Elkins-Tanton, 2007). The Ross Sea Region (namely, Northern Victoria Land and the Ross Sea) is located within the WARS, one of the world's most extensive and intensely stretched continental rifts, and it has been affected since the late Cretaceous by significant lithospheric thinning. The region is characterized by an extensional rifting phase, or strike-slip to transtensional tectonic regime, that has led to the formation of regularly spaced NW-SE right-lateral strike-slip faults and N-S striking basins, such as the Adare and Victoria Land Basins (Salvini et al., 1997; Rocchi et al., 2003; Storiti et al., 2007). Moreover, the studied area is known to lie on presumably hot and young lithospheric mantle (Nardini et al., 2009; Melchiorre et al., 2011; Perinelli et al., 2011). Therefore, it is not appropriate to apply the delamination/detachment of lithospheric mantle model, which is favored in a relatively cold, possibly old, and thick lithospheric mantle under a convergent tectonic setting, to explain asthenospheric upwelling in the geodynamic scenario of the Ross Sea Region. Instead, small-scale convective flow driven by thermal contrasts associated with steps in lithospheric thickness at the boundary of cratonic continent and ocean appears to have been a driving mechanism for the Cenozoic NVL volcanism (e.g., Nardini et al., 2009; Armienti and Perinelli, 2010; Perinelli et al., 2011).

Since Eocene there has been hot mantle flow under the extended, thinned part of the WARS, directed towards the thick Antarctic craton (Faccenna et al., 2008), which is considered to have built up the heat to warm the mantle at the edge (western rift shoulder) of the thick Antarctic lithosphere. The continuing mantle flow toward thick craton accompanying hot asthenospheric melts may trigger local melting of metasomatized veined lithospheric mantle and produce higher degree of partial melting magmas in the western rift shoulder compared to lower degrees of magmas within rift setting. Partial melting, mixing, and averaging of melts with different proportions of metasomatized lithospheric and

asthenospheric mantle may give rise to the range of magma compositions seen in the Cenozoic NVL magmatism. The isotopic variation in MMVF and Terror Rift magmas also appears to be linked to the difference in degree of partial melting. In case of a low degree of melting of Terror Rift magma, it could preferentially tap enriched vein material with HIMU signature, which is the most commonly found mantle signature, in NVL. In contrast, the higher degree of partial melting of the MMVF A and B magmas can be explained by the more extensive sampling area of the heterogeneous mantle domain. As a consequence, the HIMU signature of the MMVF A and B lavas is probably diluted compared with that of the Terror Rift submarine lavas.

6. CONCLUSIONS

(1) The Terror Rift submarine and MMVF Group A and B samples are alkaline, ranging from basanite to trachybasalt, and show the OIB-like patterns of trace element distribution, with a prominent depletion in K and Pb. Compared with the MMVF Group A and B basalts, the Terror Rift submarine samples have lower SiO₂ and Al₂O₃, higher MgO and CaO, higher ratios of more to less incompatible elements (La/Yb, La/Sm, Nb/Y, Th/Yb, and U/Pb), and more radiogenic Pb and Nd and less radiogenic Sr isotopic compositions.

(2) The K/Ar ages suggest that MMVF Group A and B and Terror Rift submarine lavas represent products of three distinct magmatic episodes. MMVF Group A samples show the youngest ages, ranging from 0.1 to 0.3 Ma, Group B samples have the oldest ages, from 1.25 to 1.34 Ma, and the Terror Rift samples have ages of 0.46–0.57 Ma.

(3) REE modeling and the isotopic compositions of the Terror Rift samples suggest that they were derived from low (1–2%) partial melting of an amphibole-bearing garnet peridotite mantle source with preferential melting of a HIMU-like component in metasomatized lithospheric mantle. In contrast, the geochemical characteristics of the MMVF Group A and B basalts reflect the large geographic scale of sampling (higher degrees (2–5%) of melting) of heterogeneous lithospheric mantle and could be explained by the consequence of mixing and averaging of melts involving depleted MORB-like, HIMU-like, and EMI-like components.

(4) We consider that edge-driven convective flow under the thinned lithospheric mantle of NVL toward the thick Antarctic Craton may have allowed upwelling of hot asthenospheric melts and triggered local melting of metasomatized veined lithospheric mantle.

ACKNOWLEDGMENTS: This study was supported by the KOPRI projects (PM15030, PE15050). We would like to thank J.M. Back (mass spectrometry), S.H. Han (ICP-MS) and S.A. Ha (isotope chemistry) for their assistance with analytical work. We acknowledge editor Kyoungwon Kyle Min and two anonymous reviewers for their constructive comments that improved the manuscript.

REFERENCES

- Aldanmaz, E., Pearce, J.A., Thirlwall, M.F., and Mitchell, J.G., 2000, Petrogenetic evolution of late Cenozoic, post-collision volcanism in western Anatolia, Turkey. *Journal of Volcanology and Geothermal Research*, 102, 67–95.
- Aldanmaz, E., Köprübaşı, N., Güner, Ö.F., Kaymakçı, N., and Gourgaud, A., 2006, Geochemical constraints on the Cenozoic, OIB-type alkaline volcanic rocks of NW Turkey: implications for mantle sources and melting processes. *Lithos*, 86, 50–76.
- Armienti, P. and Baroni, C., 1999, Cenozoic climatic change in Antarctica recorded by volcanic activity and landscape evolution. *Geology*, 27, 617–620.
- Armienti, P. and Perinelli, C., 2010, Cenozoic thermal evolution of lithospheric mantle in northern Victoria Land (Antarctica): Evidences from mantle xenoliths. *Tectonophysics*, 486, 28–35.
- Becker, H., 1996, Crustal trace element and isotopic signatures in garnet pyroxenites from garnet peridotite massifs from lower Austria. *Journal of Petrology*, 37, 785–810.
- Behrendt, J.C., 1999, Crustal and lithospheric structure of the West Antarctic Rift System from geophysical investigations: A review. *Global and Planetary Change*, 23, 25–44.
- Behrendt, J.C., LeMasurier, W.E., Cooper, A.K., Tessensohn, F., Tréhu, A., and Damaske, D., 1991, Geophysical studies of the West Antarctic Rift System. *Tectonics*, 10, 1257–1273.
- Chand, S., Radhakrishna, M., and Subrahmanyam, C., 2001, India-East Antarctica conjugate margins: Rift-shear tectonic setting inferred from gravity and bathymetry data. *Earth and Planetary Science Letters*, 185, 225–236.
- Chazot, G., Menzies, M.A., and Harte, B., 1996, Determination of partition coefficients between apatite, clinopyroxene, amphibole, and melt in natural spinel lherzolites from Yemen: implications for wet melting of the lithospheric mantle. *Geochimica et Cosmochimica Acta*, 60, 423–437.
- Choo, M.K., Lee, M.J., Lee, J.I., Kim, K.H., and Parl, K.-H., 2012, Geochemistry and Sr-Nd-Pb isotopic constraints on the petrogenesis of Cenozoic lavas from the Pali Aike and Morro Chico area (52°S), southern Patagonia, South America. *Island Arc*, 21, 327–350.
- Class, C. and Goldstein, S.L., 1997, Plume–lithosphere interactions in the ocean basins; constraints from the source mineralogy. *Earth and Planetary Science Letters*, 150, 245–260.
- Coltorti, M., Beccaluva, L., Bonadiman, C., Faccini, B., Ntaflou, T., and Siena, F., 2004, Amphibole genesis via metasomatic reaction with clinopyroxene in mantle xenoliths from Victoria Land, Antarctica. *Lithos*, 75, 115–139.
- Cook, C., Briggs, R.M., Smith, I.E.M., and Maas, R., 2005, Petrology and geochemistry of intraplate basalts in the south Auckland volcanic field, New Zealand: evidence for two coeval magma suites from distinct sources. *Journal of Petrology*, 46, 473–503.
- Cooper, A.F., Adam, L.J., Coulter, R.F., Eby, G.N., and McIntosh, W.C., 2007, Geology, geochronology and geochemistry of a basaltic volcano, White Island, Ross Sea, Antarctica. *Journal of Volcanology and Geothermal Research*, 165, 189–216.
- DePaolo, D.J. and Daley, E.E., 2000, Neodymium isotopes in basalts of the southwest Basin and Range and lithospheric thinning during continental extension. *Chemical Geology*, 169, 157–185.
- Elikins-Tanton, L.T., 2007, Continental magmatism, volatile recycling, and heterogeneous mantle caused by lithospheric gravitational instabilities. *Journal of Geophysical Research*, 112, B03405. doi: 10.1029/2005JB004072
- Finn, C.A., Dietmar Müller, R., and Panter, K.S., 2005, A Cenozoic diffuse alkaline magmatic province (DAMP) in the southwest Pacific province without rift or plume origin. *Geochemistry, Geophysics, Geosystems*, 6, Q02005. doi:10.1029/2004GC000723
- Fitzgerald, P.G. and Stump, E., 1997, Cretaceous and Cenozoic episodic denudation of the Transantarctic Mountains, Antarctica: New constraints from apatite fission track thermochronology in the Scott Glacier region. *Journal of Geophysical Research*, 102, 7747–7765.
- Foley, S., 1991, High-pressure stability of the fluor- and hydroxy-end-members of paragasite and K-rich richterite. *Geochimica et Cosmochimica Acta*, 55, 2689–2694.
- Furman, T. and Graham, D., 1999, Erosion of lithospheric mantle beneath the East African Rift system: geochemical evidence from the Kivu volcanic province. *Lithos*, 48, 237–262.
- Gallagher, K. and Hawkesworth, C., 1992, Dehydration melting and the generation of Continental Flood Basalts. *Nature*, 358, 57–59.
- Hart, S.R., Blusztajn, J., and Craddock, C., 1995, Cenozoic volcanism in Antarctica: Jones Mountains and Peter I Island. *Geochimica et Cosmochimica Acta*, 59, 3379–3388.
- Hart, S.R., Blusztajn, J., LeMasurier, W.E., and Rex, D.C., 1997, Hobbs Coast Cenozoic volcanism: implications for the West Antarctic rift system. *Chemical Geology*, 139, 223–248.
- Hawkesworth, C.J. and Gallagher, K., 1993, Mantle hotspots, plumes and regional tectonics as causes of intraplate magmatism. *Terra Nova*, 5, 552–559.
- Hoernle, K., White, J.D.L., van den Bogaard, P., Hauff, F., Coombs, D.S., Werner, R., Timm, C., Garbe-Schonberg, D., Reay, A., and Cooper, A.F., 2006, Cenozoic intraplate volcanism on New Zealand: upwelling induced by lithospheric removal. *Earth and Planetary Science Letters*, 248, 335–352.
- Hofmann, A.W., Jochum, K.P., Seufert, M., and White, W.M., 1986, Nb and Pb in oceanic basalts: new constraints on mantle evolution. *Earth and Planetary Science Letters*, 79, 33–45.
- Hole, M.J. and LeMasurier, W.E., 1994, Tectonic controls on the geochemical composition of Cenozoic, mafic alkaline volcanic rocks from West Antarctica. *Contribution to Mineralogy and Petrology*, 117, 187–202.
- Ishizuka, O., Taylor, R.N., Milton, J.A., and Nesbitt, R.W., 2003, Fluid–mantle interaction in an intra-oceanic arc: constraints from high-precision Pb isotopes. *Earth and Planetary Science Letters*, 211, 221–236.
- Johnson, J.S., Gibson, S.A., Thompson, R.N., and Nowell, G.M., 2005, Volcanism in the Vitim Volcanic Field, Siberia: geochemical evidence for a mantle plume beneath the Baikal Rift Zone. *Journal of Petrology*, 46, 1309–1344.
- Kyle, P.R., 1990, McMurdo Volcanic Group, Western Ross Embayment. In: LeMasurier, W.E. and Thomson, J.W. (eds.), *Volcanoes of the Antarctic Plate and Southern Oceans*. Antarctic Research Series, 48, AGU, Washington, D.C. p. 19–25.
- Kyle, P.R. and Muncy, H.L., 1989, Geology and geochronology of McMurdo volcanic group rock in the vicinity of Lake Morning, McMurdo Sound, Antarctica. *Antarctic Science*, 1, 345–350.
- Le Bas, M.J., Le Maitre, R.W., Streckeisen, A., and Zanettin, B., 1986, A chemical classification of volcanic rocks based on the Total Alkali–Silica diagram. *Journal of Petrology*, 27, 745–750.
- LeMasurier, W.E. and Landis, C.A., 1996, Mantle-plume activity recorded by low relief erosion surfaces in West Antarctica and New Zealand. *Geological Society of American Bulletin*, 108, 1450–1466.
- Lee, M.J., Lee, J.I., Kwon, S.-T., Choo, M.K., Jeong, K.-S., Cho, J.-H., and Kim, S.-R., 2011, Sr-Nd-Pb isotopic compositions of submarine alkali basalts recovered from the South Korea Plateau,

- East Sea. *Geosciences Journal*, 15, 149–160.
- Ma, G.-S.-K., Malpas, J., Xenophontos, C., Suzuki, K., and Lo, C.-H., 2011, Early Cretaceous volcanism of the Coastal Ranges, NW Syria: Magma genesis and regional dynamics. *Lithos*, 126, 290–306.
- Martin, A.P., Cooper, A.F., and Price, R.C., 2013, Petrogenesis of Cenozoic, alkalic volcanic lineages at Mount Morning, West Antarctica and their entrained lithospheric mantle xenoliths: Lithospheric versus asthenospheric mantle sources. *Geochimica et Cosmochimica Acta*, 122, 127–152.
- McCoy-West, A.J., Baker, J.A., Faure, K., and Wysoczanski, R., 2010, Petrogenesis and origins of Mid-Cretaceous continental intraplate volcanism in Marlborough, New Zealand: implications for the long-lived HIMU magmatic mega-province of the SW Pacific. *Journal of Petrology*, 51, 2003–2045.
- McDonough, W.F. and Sun, S.S., 1995, The composition of the Earth. *Chemical Geology*, 120, 223–253.
- McKenzie, D. and O’Nions, R.K., 1991, Partial melt distributions from inversion of rare earth element concentrations. *Journal of Petrology*, 32, 1021–1091.
- McKenzie, D. and Bickle, M.J., 1988, The volume and composition of melt generated by extension of the lithosphere. *Journal of Petrology*, 29, 625–679.
- Melchiorre, M., Coltorti, M., Bonadiman, C., Faccini, B., O’Reilly, S.Y., and Pearson, N.J., 2011, The role of eclogite in the rift-related metasomatism and Cenozoic magmatism of Northern Victoria Land, Antarctica. *Lithos*, 124, 319–330.
- Müller, P., Schmidt-Thom, M., Kreuzer, H., Tessensohn, F., and Vetter, U., 1991, Cenozoic peralkaline magmatism at the western margin of the Ross Sea, Antarctica. *Memorie Società Geologica Italiana*, 46, 315–336.
- Nagao, K., Nishido H., Itaya, T., and Ogata, K., 1984, An age Determination by K-Ar Method. *The Bulletin of the Hiruzen Research Institute*, 9, 19–38.
- Nagao, K., Ogata, A., Miura, Y.N., and Yamaguchi, K., 1996, Ar isotope analysis for K- mass spectrometers I: Isotope dilution method. *Journal of Mass Spectrometry Society of Japan*, 44, 36–61.
- Nardini, I., Armienti, P., Rocchi, S., Dallai, L., and Harrison, D., 2009, Sr-Nd-Pb-He-O isotope and geochemical constraints on the genesis of Cenozoic magmas from the West Antarctic Rift. *Journal of Petrology*, 50, 1359–1375.
- Orihashi, Y., Naranjo, J.A., Motoki, A., Sumino, H., Hirata, D., Anma, R., and Nagao, K., 2004, Quaternary volcanic activity of Hudson and Lautaro volcanoes, Chilean Patagonia: New constraints from K-Ar ages. *Revista Geologica de Chile*, 31, 207–224.
- Panter, K.S., Hart, S.R., Kyle, P.R., Blusztajn, J., and Wilch, T.I., 2000, Geochemistry of Late Cenozoic basalts from the Cray Mountains: Characterization of mantle sources in Marie Byrd Land, Antarctica. *Chemical Geology*, 165, 215–241.
- Panter, K.S., Blusztajn, J., Hart, S.R., Kyle, P.R., Esser, R., and McIntash, W.C., 2006, The origin of HIMU in the SW Pacific: evidence from intraplate volcanism in southern New Zealand and Subantarctic islands. *Journal of Petrology*, 47, 1673–1704.
- Perinelli, C., Armienti, P., and Dallai, L., 2006, Geochemical and O-isotope constraints on the evolution of lithospheric mantle in the Ross Sea rift area (Antarctica). *Contributions to Mineralogy and Petrology*, 151, 245–266.
- Perinelli, C., Armienti, P., and Dallai, L., 2011, Thermal evolution of the lithosphere in a rift environment as inferred from the geochemistry of mantle cumulates, Northern Victoria Land, Antarctica. *Journal of Petrology*, 52, 665–690.
- Rocchi, S., Armienti, P., D’Orazio, M., Tonarini, S., Wijbrans, J.R., and Di Vincenzo, G., 2002, Cenozoic magmatism in the western Ross Embayment: Role of mantle plume versus plate dynamics in the development of the West Antarctic Rift System. *Journal of Geophysical Research*, 107, ECV 5-1–ECV 5-22. doi:10.1029/2001JB000515
- Rocchi, S., Storti, F., Di Vincenzo, G., and Rossetti, F., 2003, Intraplate strike-slip tectonics as an alternative to mantle plume activity for the Cenozoic rift magmatism in the Ross Sea region, Antarctica. In: Storti, F., Holdsworth, R.E., and Salvini, F. (eds.), *Intraplate Strike-Slip Deformation Belts*. Geological Society Special Publication, 210, London, p. 145–158.
- Rocchi, S., Armienti, P., and Di Vincenzo, G., 2005, No plume, no rift magmatism in the West Antarctic Rift. In: Foulger, G.R., Natland, J.H., Presnall, D.C., and Anderson, D.L. (eds.), *Plates, Plumes, and Paradigms*. Geological Society of America Special Papers, 388, p. 435–447.
- Rocholl, A., Stein, M., Molzahan, M., Hart, S.R., and Wörner, G., 1995, Geochemical evolution of rift magmas by progressive tapping of stratified mantle source beneath the Ross Sea rift, Northern Victoria Land, Antarctica. *Earth and Planetary Science Letters*, 131, 207–224.
- Ryan, J.G. and Kyle, P.R., 2004, Lithium abundance and lithium isotope variations in mantle sources: insights from intraplate volcanic rocks from Ross Island and Marie Byrd Land (Antarctica) and other oceanic islands. *Chemical Geology*, 212, 125–142.
- Salvini, F., Brancolini, G., Buseti, M., Storti, F., Mazzarini, F., and Coren, F., 1997, Cenozoic geodynamics of the Ross Sea Region, Antarctica: Crustal extension, intraplate strike-slip faulting and tectonic inheritance. *Journal of Geophysical Research*, 102, 24669–24696.
- Schott, B. and Schmeling, H., 1998, Delamination and detachment of a lithospheric root. *Tectonophysics*, 296, 225–247.
- Schott, B., Yuen, D.A., and Schmeling, H., 2000, The significance of shear heating in continental delamination. *Physics of the Earth Planetary Interiors*, 118, 273–290.
- Shaw, D.M., 1970, Trace element fractionation during anatexis. *Geochimica et Cosmochimica Acta*, 34, 237–243.
- Sprung, P., Schuth, S., Münker, C., and Hoke, L., 2007, Intraplate volcanism in New Zealand: the role of fossil plume material and variable lithospheric properties. *Contribution to Mineralogy and Petrology*, 153, 669–687.
- Storey, B.C., Leat, P.T., Weaver, S.D., Pankhurst, R.J., Bradshaw, J.D., and Kelley, S., 1999, Mantle plumes and Antarctica–New Zealand rifting: evidence from mid-Cretaceous mafic dykes. *Journal of the Geological Society*, London, 156, 659–671.
- Storti, F., Rossetti, F., Salvini, F., and Phipps Morgan, J., 2007, Intraplate termination of transform faulting within the Antarctic continent. *Earth and Planetary Science Letters*, 260, 115–126.
- Stracke, A., 2012, Earth’s heterogeneous mantle: a product of convection-driven interaction between crust and mantle. *Chemical Geology*, 330–331, 274–299.
- Tang, Y.-J., Zhang, H.-F., and Ying, J.-F., 2006, Asthenosphere-lithospheric mantle interaction in an extensional regime: Implication from the geochemistry of Cenozoic basalts from Taihang Mountains, North China Craton. *Chemical Geology*, 233, 309–327.
- Taylor, S.R. and McLennan S.M., 1985, *The Continental Crust: Its Composition and Evolution*. Blackwell, Oxford, 312 p.
- Timm, C., Hoernle, K., Bogaard, P.V.D., Bindemann, I., and Weaver, S.D., 2009, Geochemical evolution of intraplate volcanism at Banks Peninsula, New Zealand: interaction between asthenospheric and lithospheric melts. *Journal of Petrology*, 50, 989–1023.
- Timm, C., Hoernle, K., Werner, R., Hauff, F., Bogaard, P.V.D., White, J., Mortimer, N., and Garbe-Schnberg, D., 2010, Temporal and

- geochemical evolution of the Cenozoic intraplate volcanism of Zealandia. *Earth Science Reviews*, 98, 38–64.
- Tonarini, S., Rocchi, S., Armienti, P., and Innocenti, F., 1997, Constraints on timing of Ross Sea rifting inferred from Cenozoic intrusions from northern Victoria Land, Antarctica. In: Ricci, C.A. (ed.), *The Antarctic Region: Geological Evolution and Processes*. Terra Antarctica publication, Siena, p. 511–521.
- Trønnes, R.G., 2002, Stability range and decomposition of potassic richterite and phlogopite end members at 5–15 GPa. *Mineralogy and Petrology*, 74, 129–148.
- Vlastélic, I., Dosso, L., Bougault, H., Aslanian, D., Géli, L., Etou-bleau, J., Bohn, M., Joron, J.-L., and Bollinger, C., 2000, Chemical systematics of an intermediate spreading ridge: The Pacific–Antarctic Ridge between 56°S and 66°S. *Journal of Geophysical Research*, 105, 2915–2936.
- Weinstein, Y., Navon, O., Altherr, R., and Stein, M., 2006, The role of lithospheric mantle heterogeneity in the generation of Plio–Pleistocene alkali basaltic suites from NW Harrat Ash Shaam (Israel). *Journal of Petrology*, 47, 1017–1050.
- Willbold, M. and Stracke, A., 2010, Formation of enriched mantle components by recycling of upper and lower continental crust. *Chemical Geology*, 276, 188–197.
- Wilson, M. and Patterson, R., 2001, Intraplate magmatism related to short-wavelength convective instabilities in the upper mantle: evidence from the Tertiary–Quaternary volcanic province of western and central Europe. In: Ernst, R.E. and Buchan, K.L. (eds.), *Mantle Plumes: Their Identification Through Time*. Geological Society of America Special Paper 352, Boulder, Colorado, p. 37–58.
- Woodhead, J.D., Volker, F., and McCulloch, M.T., 1995, Routine lead isotope determinations using a lead-207–lead-204 double spike: a long-term assessment of analytical precision and accuracy. *Analyst*, 120, 35–39.
- Yan, J. and Zhao, J.X., 2008, Cenozoic alkali basalts from Jingpohu, NE China: the role of lithosphere–asthenosphere interaction. *Journal of Asian Earth Sciences*, 33, 106–121.
- Zindler, A. and Hart, S.R., 1986, Chemical geodynamics. *Annual Reviews of Earth Planetary Sciences*, 14, 493–571.

Manuscript received June 8, 2015

Manuscript accepted October 14, 2015